

Linköping University Post Print

Influence of exposure to 980 nm laser radiation on the luminescence of Si: Er/O light-emitting diodes

Amir Karim, Chun-Xia Du and Göran Hansson

N.B.: When citing this work, cite the original article.

Original Publication:

Amir Karim, Chun-Xia Du and Göran Hansson, Influence of exposure to 980 nm laser radiation on the luminescence of Si: Er/O light-emitting diodes, 2008, JOURNAL OF APPLIED PHYSICS, (104), 12, 123110.

<http://dx.doi.org/10.1063/1.3050316>

Copyright: American Institute of Physics

<http://www.aip.org/>

Postprint available at: Linköping University Electronic Press

<http://urn.kb.se/resolve?urn=urn:nbn:se:liu:diva-16512>

Influence of exposure to 980 nm laser radiation on the luminescence of Si:Er/O light-emitting diodes

A. Karim,^{a)} C.-X. Du, and G. V. Hansson

Department of Physics, Chemistry and Biology, Linköping University, SE-58183 Linköping, Sweden

(Received 19 May 2008; accepted 4 November 2008; published online 19 December 2008)

Erbium (Er) codoping with oxygen (O) in Si is a well-known method for producing electroluminescent material radiating at 1.54 μm through a 4*f* shell transition of Er³⁺ ions. In this work the influence of exposure to 980 nm radiation on the electroluminescence (EL) of reverse biased Si:Er/O light-emitting diodes (LEDs), which give a strong room temperature 1.54 μm intensity, is presented and discussed. All the device layers, including Er/O doped Si sandwiched between two Si_{0.82}Ge_{0.18} layers, have been grown on silicon on insulator substrates using molecular beam epitaxy and processed to fabricate edge emitting Si:Er/O waveguide LEDs. Electromagnetic mode confinement simulations have been performed to optimize the layer parameters for waveguiding. The temperature dependence of the 1.54 μm EL intensity exhibits an abnormal temperature quenching with a peak near -30 °C, and at -160 °C it has decreased by a factor of 5. However, irradiating the devices with a 980 nm laser gives an enhancement of the 1.54 μm EL intensity, which is more dramatic at low temperatures (e.g., -200 °C) where the quenched EL signal is increased up to almost the same level as at room temperature. The enhancement of the EL intensity is attributed to the photocurrent generated by the 980 nm laser, reducing the detrimental avalanche current. © 2008 American Institute of Physics. [DOI: 10.1063/1.3050316]

I. INTRODUCTION

There has been a large increase in activity in the field of Si photonics in the current decade for making Si emit light more efficiently in connection with the potential for accomplishing the communication demands of the future era. The major driving force behind the attempts of obtaining silicon light emitters is to fabricate a strong light source (laser) based on Si to integrate it with other Si based optical and electrical components for realizing optical communication.¹ Despite the fact that Si is capable of modulating and detecting light, obtaining optical gain or lasing in Si is still one of the fundamental challenges in the field of Si photonics because bulk Si is an indirect bandgap semiconductor material. In order to resolve this technical inability of Si, several approaches have been investigated. Light emission from Si, although with very low intensity compared to III-V materials, has been realized through different ways; particularly a great amount of work has been done on optically active doping of Er into the Si matrix for light emission. Nevertheless the work on Si based optical devices has taken an increased pace in the present decade. Two of the significant accomplishments in that respect include the demonstration of a continuous-wave Raman Si laser^{2,3} and a hybrid silicon laser.⁴ However both of these are based on indirect approaches that involve certain limitations. The direct approach of obtaining an electrically pumped fully Si based gain element has yet to be realized. One of the direct and fundamental approaches include Er and O doped epitaxially grown Si layers to fabricate LEDs, which may be used to design an electrically pumped Si laser. The role of O codoping is to

enhance the solid solubility limit of Er in Si, as well as to improve the formation of optically active Er/O centers in Si and thus increase the luminescence.⁵⁻⁷

The rare earth element Er in its Er³⁺ state can give a very useful radiation of 1.54 μm wavelength from the intra-4*f* shell transition between the first excited state ⁴I_{13/2} and the ground state ⁴I_{15/2}.⁸⁻¹⁰ The importance of this wavelength is due to the fact that it falls in the minimum loss window of transmission in optical fibers. Furthermore, the Si:Er/O material system can be integrated with the devices manufactured by the well established Si process technology. Si:Er/O light-emitting diodes (LEDs) emitting 1.54 μm light have been extensively studied over a period of time,¹¹⁻¹⁷ e.g., to understand the mechanism of Er³⁺ excitation for improving the efficiency of these devices. Unlike III-V LEDs, Si:Er/O LEDs are preferentially operated in reverse bias condition because it is well known that the hot electron impact excitation of Er ions in the reverse breakdown region is much more efficient as compared to Er³⁺ excitation via electron hole recombination in forward bias.^{14,15} One of the key issues in these devices is the response of their electroluminescence (EL) to temperature. Initially there were reports on strong low temperature EL that quenches drastically with increasing temperature, particularly at room temperature.¹²⁻¹⁴ Later on there have also been reports on successful room temperature EL of Si:Er/O LEDs under reverse bias but with a significant decrease of intensity with decreasing temperature.¹⁸⁻²⁰ This phenomenon is referred to as the abnormal temperature quenching of the EL and it has been attributed in one way or another to the reverse breakdown mechanism of diodes.^{18,21}

In the present paper, studies of the influence of 980 nm laser irradiation on the luminescence characteristics of Si:Er/O light-emitting structures grown on silicon on insula-

^{a)}Electronic mail: amkar@ifm.liu.se.

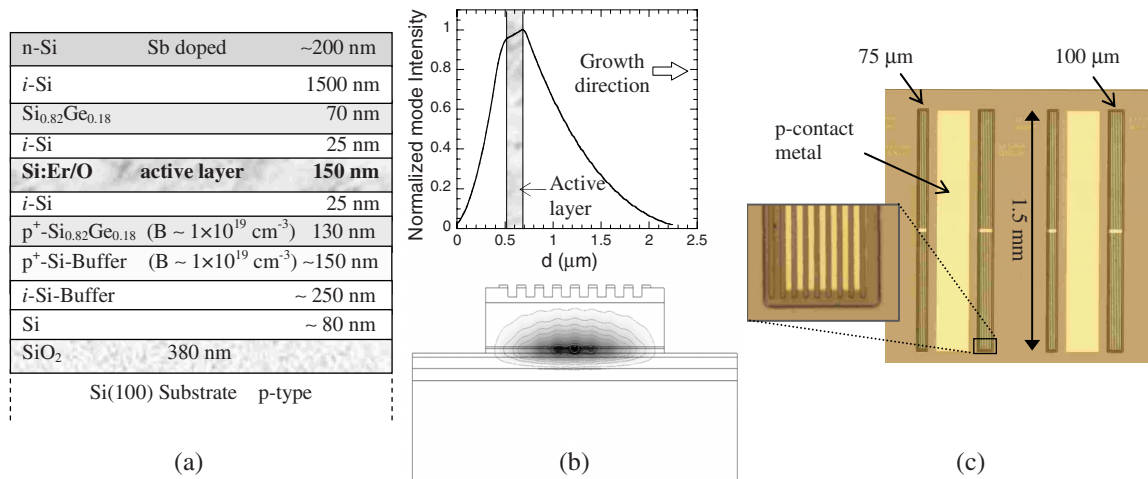


FIG. 1. (Color online) (a) Schematic device layer structure. (b) Mode confinement result using FEMLAB. (c) Optical microscope image of a set of processed devices. The inset shows the metal stripes of the n -contact on top of a mesa.

tor (SOI) are reported. The large effects on the EL of Si:Er/O LEDs by the 980 nm laser, measured at room temperature and low temperatures, are discussed. Results of EL, transmission electron microscopy (TEM), current-voltage (IV), and secondary ion mass spectrometry (SIMS) are presented. Simulation results of electromagnetic mode confinement in the present Si/SiGe waveguides on SOI are also presented.

II. EXPERIMENTAL DETAILS

The light-emitting device structures were epitaxially grown using a VG V80 molecular beam epitaxy (MBE) system for the purpose of getting a light-emitting waveguide structure on SOI substrates. The SOI wafers used contained a 400 nm thick SiO₂ layer on a Si substrate covered by an 80 nm thick Si (100) single crystal. After performing the usual *in situ* high temperature (820 °C) cleaning step, a 250 nm thick Si buffer layer was grown, followed by a 150 nm thick p⁺-Si layer with a boron (B) concentration of $1 \times 10^{19} \text{ cm}^{-3}$. After that a p⁺-SiGe layer with 18% Ge and the same B concentration was grown, which also served as p-contact layer. Then a 25 nm thick layer of i-Si was grown before the 150 nm thick active layer of Er/O doped Si. A schematic picture of the device layers is shown in Fig. 1(a). For O doping we used a background pressure of O gas controlled by a mass spectrometer. The function of the p⁺-SiGe layer and the intrinsic layer is related to the hot electron impact excitation of Er³⁺ ions under reverse bias, as explained in more detail in Refs. 22 and 23 where Si:Er/O light emitters working on the same principle were described. However, unlike in Refs. 22 and 23, in the present devices a cap layer of i-Si was also grown before the n⁺ (Sb) doped contact layer for optical mode confinement purposes.

The future goal regarding these devices is to fabricate a cavity for obtaining an electrically pumped Si laser. Therefore, 1.5 mm long mesas with two different widths of 75 and 100 μm were designed. One important issue when producing a cavity is the confinement of optical modes. Several factors influence the mode confinement, e.g., the size of the cavity, spacer layer thickness, SiGe layers, etc. However the fact that the device layers are grown on SOI itself is a crucial

factor for mode confinement. Simulations were performed for the 1.54 μm optical mode confinement using the software called FEMLAB, and the device structure parameters were optimized. Figure 1(b) shows schematically one optimized structure with the optical mode confined at the active layer. By choosing two SiGe layers of different layer thicknesses (70 and 130 nm), sandwiching the active layer, we could increase the magnitude of mode intensity confined in the active layer, which can be seen in the intensity profile taken across the device in Fig. 1(b). It is well known that metal and, to some extent, highly doped layers are detrimental for the mode confinement, which is why an intrinsic Si spacer layer is needed to separate the contact metal from the active layer. From simulations it is realized that a spacer layer of $>1 \mu\text{m}$ thickness would lead to the 1.54 μm optical modes successfully confined at the active layer. The metal (Al) layer was modified to be 5 μm wide stripes with 0.3 μm deep and 5 μm wide trenches in between, along the 1.5 mm length of the devices, which improved the conditions by forcing the modes away from the metal contact. This design also allows measurements of light emission from the surface of the devices as well as possibilities for studying the influence of optical pumping on the device characteristics.

Due to the fact that the structures are grown on SOI substrates, the device processing is more demanding as compared to the previously studied structures on Si. In the SOI case one must take both the n - and p -contacts from the top, hence we need to fabricate mesas with sides etched precisely down to the p⁺-SiGe layer. One advantage in this regard was that the p⁺-SiGe also serves as an etch stop during wet etching with KOH solution. Using conventional photolithography with multiple masks we fabricated 1.5 mm long mesas with two different widths of 75 and 100 μm. Figure 1(c) shows top view images taken by optical microscope of a set of devices after all the processing steps.

EL measurements were performed using a conventional lock-in technique, with devices operated in reverse bias and using a Ge detector to detect the emitted light in the edge emission geometry. Measurements included EL spectra, EL intensity versus current, EL versus temperature, etc., for both

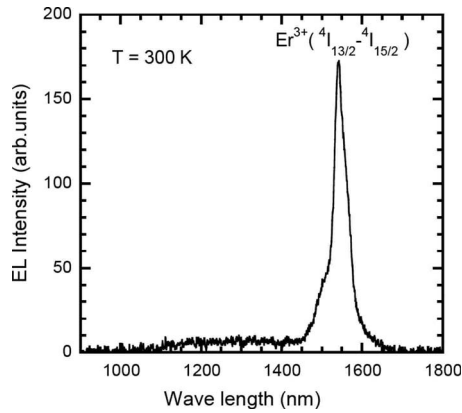


FIG. 2. EL spectrum for a Si:Er/O light-emitting device (sample F) at 2.6 A/cm^2 reverse current density.

surface emission and edge emission. In order to study the influence of the 980 nm laser on the luminescence properties of these devices, the EL setup was complemented with the possibility to expose the devices to laser radiation. The measurements include studies of the influence of both a 980 and a 1064 nm laser incident on the device surface from top on the edge emitted EL versus reverse current at different temperatures. SIMS measurements were performed to determine the concentrations of Er, O, Ge, B, and Sb in the grown device structures.

III. RESULTS AND DISCUSSION

The devices presented were aimed at having tunneling breakdown behavior at room temperature as they were operated at reverse biased breakdown conditions. However, at lower temperatures and high bias there was a gradual onset of avalanche breakdown that was evident from the temperature response of the electrical properties. Nevertheless, strong EL intensity at $1.54 \mu\text{m}$, coming from the intra-4f shell transition of Er^{3+} ions in the silicon matrix, is observed in these devices. A typical EL spectrum, taken at room temperature in edge emission geometry, is shown in Fig. 2 for 3 mA driving current. The spectrum shows a sharp peak at $1.54 \mu\text{m}$ and a fairly low broadband emission, e.g., compared to previous samples grown on Si substrates.

The EL intensity at $1.54 \mu\text{m}$ versus temperature for different reverse currents is shown in Fig. 3, covering a temperature range between room temperature and $-160 \text{ }^\circ\text{C}$. An abnormal temperature quenching of the $1.54 \mu\text{m}$ EL intensity of Er^{3+} is observed with a peak near $-30 \text{ }^\circ\text{C}$ depending on the drive current, and a four to five times decrease from the peak value to $-160 \text{ }^\circ\text{C}$. The IV curves, not shown here, revealed the tunneling type of breakdown at higher temperatures and avalanche breakdown at low temperatures. Similar as in Ref. 18 this temperature quenching is attributed to the type of breakdown mechanism that is generating the reverse current, with a crossover from tunneling dominated region at higher temperatures to an avalanche dominated region at low temperatures. In this study as well as in Ref. 18 the devices have a tunneling diode design with an electron injector layer of SiGe, and they operate in reverse bias where the electrical pumping is realized by hot electron impact excitation of the

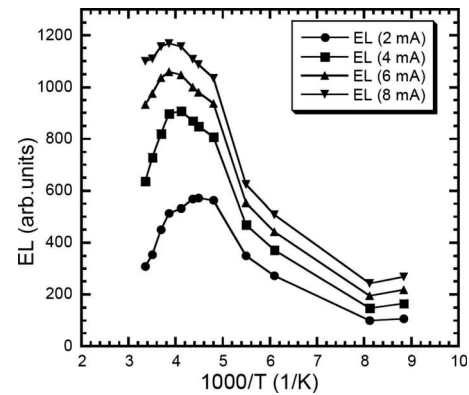


FIG. 3. EL intensity of $1.54 \mu\text{m}$ vs temperature in the range from room temperature to $-160 \text{ }^\circ\text{C}$ for different reverse currents.

Er^{3+} ions by the tunneled electrons. Based on this description it is reasonable to state that in these particular devices, the larger is the contribution of tunneling current to the total reverse current, the more Er^{3+} ions are excited, leading to a higher EL intensity. In contrast, low energy electrons generated in avalanche breakdown have a relatively lower probability of exciting Er^{3+} ions. There is also an enhancement of competing nonradiative Auger de-excitation processes due to the presence of larger number of low energy carriers generated during the ionization process, hence giving a low EL intensity.

Shmagin *et al.*²¹ also reported anomalous temperature dependence and they associated it with the changes in the uniformity of the p - n junction breakdown. However, first their diodes have a slightly different layer structure compared to our structures, and second they connected the temperature quenching of EL with the inhomogeneity increase in the current flow across the junction at breakdown, based on the visible light distribution observed in an optical microscope. In contrast to that, in our case the visible part of the broad background emission was very weak and without bright spots. Hence our devices might not exhibit the filament model presented by Shmagin *et al.*²¹ In addition to that, the measurements of the influence of 980 nm laser irradiation on the luminescence of our devices support the connection of abnormal temperature quenching with the crossover from tunneling to avalanche breakdown regime.

The concentrations of Er and O play an important role for the EL intensity at $1.54 \mu\text{m}$ from Si:Er/O LEDs. Detailed studies about the influence of Er and O concentrations, measured by SIMS, on EL properties of Si:Er/O devices have been made, some results of which have been reported elsewhere.²³ In Fig. 4 we have replotted the Er and O concentration information of Fig. 3(a) in Ref. 23 showing the earlier grown samples A, B, C, D, and E together with two of the recently grown Si:Er/O waveguide LED structures on SOI samples F and G. All the samples shown were also studied using TEM for microstructure analysis. As was reported in Ref. 23, samples with Er and O concentrations below the dotted curve in Fig. 4 contain planar type of precipitates, which are optically active. For concentrations above the dashed line there have been observations of optically inactive round type of precipitates. Hence the recently

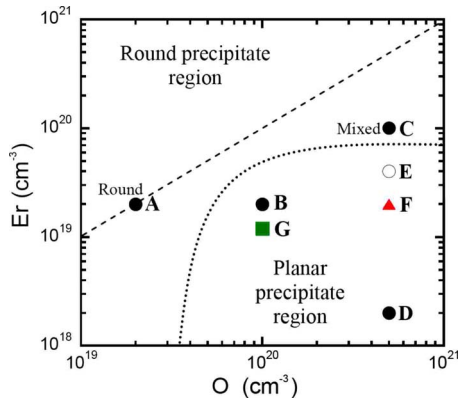


FIG. 4. (Color online) Diagram showing Er and O concentrations for different samples together with information about the microstructure. Samples A–E were previously grown (Ref. 23), whereas samples F and G are recently grown on SOI wafers.

grown samples presented in this report are within the region of planar precipitates, which was confirmed with cross section scanning TEM (STEM) analysis.

An overview of the grown layers in samples F and G, obtained by Z-contrast STEM, is shown in Fig. 5. All the layers are labeled accordingly in the micrographs, particularly the active layer of Si:Er/O sandwiched between two brighter contrast layers of SiGe. From the micrographs we can see that the growth of the layers was successfully performed on SOI based on the structural quality. The roughness in the upper SiGe layer in sample F is a consequence of faceted growth, mainly due to O, of the Er/O doped Si layer below it. On the other hand, sample G with a relatively lower doping level of O and Er does not show any sign of roughness in the second SiGe layer. This is an issue of concern for waveguiding cavities because roughness/defects may increase the light scattering losses. Nevertheless, devices fabricated from both the samples give a strong EL intensity at 1.54 μm . The roughness at the top of the n^+ -Si contact layer in both samples is due to stacking faults introduced by Sb doping, which are presently difficult to avoid but they are not detrimental. Lattice resolution images obtained (not shown here) at different interfaces including the SOI wafer and buffer layer interface showed continuous crystal epitaxy across all grown interfaces.

It is well known for Er doped fiber amplifiers that optical pumping with 980 nm light is quite efficient as this corre-

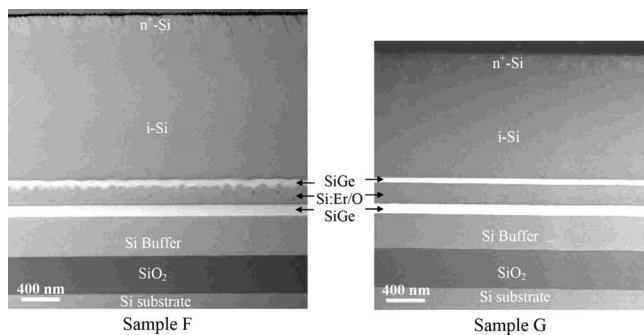


FIG. 5. Z-contrast STEM micrographs showing overviews of Si:Er/O layer structures in samples F and G.

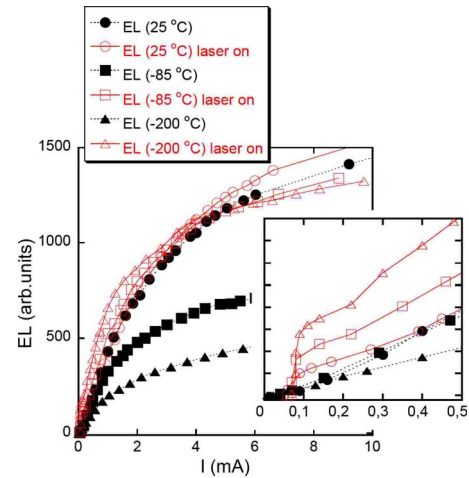


FIG. 6. (Color online) EL peak intensity at 1.54 μm vs current of Si:Er/O LED in edge emission geometry at 25, -80 , and -200 $^{\circ}\text{C}$, showing the influence of 980 nm laser irradiation. The range below 0.5 mA is replotted in the inset for clarity.

sponds to excitation of the Er ions to the second excited level;²⁴ therefore we used a strong 980 nm laser to study any possibility of optical pumping in these structures together with electrical pumping. Here it is important to mention that all the measured devices have almost 50% of the device surface open for the incident light [inset in Fig. 1(c)]. When these devices were exposed to continuous 980 nm laser light, while they were operated in the reverse biased condition in pulsed mode, there were interesting changes in the EL intensity at 1.54 μm . Figure 6 shows the EL intensity versus current of a Si:Er/O waveguide LED on SOI measured in the edge emission geometry at three different temperatures (at 25, -80 , and -200 $^{\circ}\text{C}$) for conditions with and without the 980 nm laser incident on the device from top.

With increasing drive current, the EL intensity increases and starts to saturate, which is a typical feature of Si:Er/O LEDs. The intensity drops as the temperature is lowered in the cases of no laser incident (all filled symbols in Fig. 6). This demonstrates the abnormal temperature quenching of EL, as shown earlier in Fig. 3. However there is an enhancement of the intensity when the laser is on, for all three temperatures (all open symbols in Fig. 6). This enhancement is smallest at room temperature (from the filled circles to open circles) and is most dramatic at the lowest temperature (from the filled triangles to open triangles). For example, at -200 $^{\circ}\text{C}$ there is an increase in the EL with a factor in the range of 1.5–8 depending on the current, when the laser illuminates the sample surface. The largest effect occurs at low currents. In the high current range, the EL(I) curves at all temperatures, for the laser on, are not very different from those at room temperature level without the laser.

In the case of 980 nm laser light incident on these devices without any bias, there was no photoluminescence observed at 1.54 μm using lock in measurements. A dc voltage was also applied during photoluminescence measurements but there was still negligible intensity. Therefore optical pumping of Er^{3+} ions cannot be the reason for the strong EL enhancement when the 980 nm radiation is incident on our devices. In order to confirm this further, we have also studied

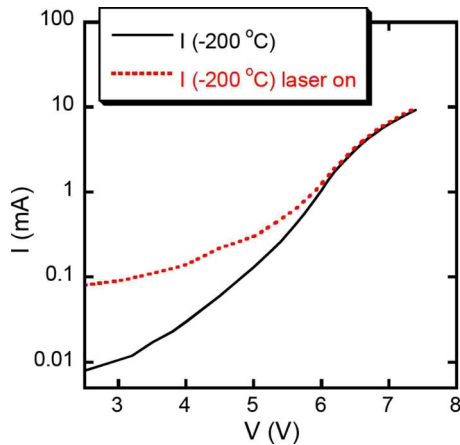


FIG. 7. (Color online) IV curves of a Si:Er/O diode in reverse bias at -200 °C showing the influence of the 980 nm laser incident on the device.

the influence of laser light with a wavelength of 1064 nm, which is nonresonant with Er^{3+} energy levels, on the EL properties. The influence of 1064 nm radiation on the EL of the same devices was identical to that of the 980 nm radiation, with no sign of direct excitation of Er during photoluminescence (PL) but a significant enhancement of the 1.54 μm EL intensity at low temperatures when the 1064 nm laser was on.

PL measurements on these layered structures were also performed with a more sensitive setup, at 2.5 K using a high-power 980 nm laser line for excitation. The results of such measurements also did not reveal any Er^{3+} related emission. This indicates that excitation to the second excited state of Er^{3+} ions, which is above Si bandgap, is not an efficient way to generate 1.54 μm radiation in the present structures.

Based on the current experimental results we propose that the EL enhancements due to the 980 and 1064 nm laser irradiations are due to the optically generated carriers leading to an additional contribution to the total reverse current. Figure 7 shows IV curves recorded at -200 °C under the same conditions as in Fig. 6, with a comparison between the IV curves with laser on (dashed curve) and without the laser on (solid curve). It is quite evident that the IV curve with the 980 nm laser on shows some extra current in the whole range. At very low applied reverse bias voltages, e.g., at 2.5 V, the current with laser on is ten times higher. We argue that, due to the extra contribution of photocurrent, the contribution of the reverse current generated by avalanche mechanism, which is detrimental for EL, is to some extent reduced. The optically generated electrons acquire kinetic energy in the reverse field, just like the tunneled electrons, and become a source of Er^{3+} excitation as well. This phenomenon is also revealed as a threshold behavior in the $EL(I)$ curves, when the 980 nm laser is on, at very low currents (open symbols in the inset of Fig. 6). Consequently the overall EL intensity is enhanced due to the 980 nm laser incident on these devices.

It is important to mention that there is also a heating effect due to the high-power 980 nm laser, which would lead to an increase in the EL at low temperatures. However, careful temperature measurements of wafers in similar experi-

mental conditions revealed that the temperature increase by the laser is not more than ~ 25 °C. Moreover the EL versus temperature curves of Fig. 3 show a rapid decrease in the EL intensity with increased temperature above ~ -30 °C, whereas in the case of laser on at room temperature there is an enhancement in EL, most evidently at high currents (>3 mA).

Comparison of $EL(I)$ curves, at different temperatures, in the case of the 980 nm laser incident (all open symbols in Fig. 6) revealed a crossover between the curves around 3 mA. At lower currents the room temperature $EL(I)$ curve is below the $EL(I)$ curve of -200 °C, which is a similar trend as normal temperature quenching, whereas above 3 mA, the -200 °C $EL(I)$ curve is the lowest, which is qualitatively similar as the abnormal temperature quenching. This behavior can be attributed to a relative increase in avalanche current at higher applied reverse bias. Although increasing the applied bias leads to the planned electron tunneling at the narrow part of SiGe bandgap, the possibility of avalanche breakdown is also enhanced. It is known that generation of avalanche current is a consequence of the multiple interband excitations, which more easily takes place at lower temperatures. Therefore the $EL(I)$ curves in Fig. 6 for laser on reveal a crossover at higher bias conditions to a region where the $EL(I)$ curve of -200 °C is lowest among the three curves. Nevertheless the intensity level for all temperatures is still higher as compared to the case with laser off. In conclusion we can say that the 980 nm laser helps to a large extent in recovering the quenched EL intensity at low temperatures in our devices, through changes in the electrical breakdown of the reverse biased diodes.

IV. CONCLUSIONS

In this contribution we have presented the results of growth, processing, structural, and optical characterizations of Si:Er/O waveguide LEDs and discussed the influence of 980 nm laser irradiation on the 1.54 μm EL. The layer structures were optimized based on mode confinement simulations and successfully grown on SOI substrates using the growth technique of MBE. The devices operated in the reverse breakdown region show strong room temperature EL intensity of 1.54 μm both from surface and edge. Measurements of the 1.54 μm EL versus temperature, covering a range from room temperature down to -160 °C, exhibit abnormal temperature quenching, with a peak near -30 °C, and at -160 °C it has decreased by a factor of 5. To investigate ways of increasing the EL intensity, measurements with 980 nm laser radiation incident on these devices have been performed. The exposure of the devices to the 980 nm laser counteracts the low temperature quenching of the 1.54 μm EL, while there is no contribution to the light emission from photoluminescence. A significant enhancement (more than 150%) of the quenched 1.54 μm EL intensity at low temperatures (-200 °C) was observed when the devices were exposed to the 980 nm laser. The recovery of the quenched EL of these devices at different temperatures due to the 980 nm laser exposure is attributed to the changes in the electrical breakdown. Due to the generation of photocur-

rent, the contribution of detrimental avalanche current is reduced and an enhancement of the 1.54 μm EL even at very small voltages ($\sim 2\text{V}$), less than the reverse breakdown voltage, is obtained.

ACKNOWLEDGMENTS

We wish to thank M. K. Linnarsson at Microelectronics and Applied Physics, Royal Institute of Technology, Sweden, for performing SIMS measurements. We also like to acknowledge K. F. Karlsson for performing low temperature PL measurements.

- ¹G. T. Reed, *Silicon Photonics* (Wiley, New York, 2004).
- ²H. Rong, R. Jones, A. Liu, O. Cohen, D. Hak, A. Fang, and M. Paniccia, *Nature (London)* **433**, 725 (2005).
- ³O. Boyraz and B. Jalali, *Opt. Express* **12**, 5269 (2004).
- ⁴A. W. Fang, H. Park, Y.-H. Kuo, R. Jones, O. Cohen, D. Liang, O. Rada, M. N. Sysak, M. J. Paniccia, and J. E. Bowers, *Mater. Today* **10**, 28 (2007).
- ⁵W.-X. Ni, K. B. Joelsson, C.-X. Du, I. A. Buyanova, G. Pozina, W. M. Chen, G. V. Hansson, B. Monemar, J. Cardenas, and B. G. Svensson, *Appl. Phys. Lett.* **70** (1997) 3383.
- ⁶A. Reittinger, J. Stimmer, and G. Abstreiter, *Appl. Phys. Lett.* **70**, 2431 (1997).
- ⁷S. Scalse, G. Franzò, S. Mirabella, M. Re, A. Terrasi, F. Priolo, E. Rimini, C. Spinella, and A. Carnera, *J. Appl. Phys.* **88**, 4091 (2000).
- ⁸D. L. Adler, D. C. Jacobson, D. J. Eaglesham, M. A. Marcus, J. L. Benton, J. M. Poate, and P. H. Citrin, *Appl. Phys. Lett.* **61**, 2181 (1992).
- ⁹H. Ennen, G. Pomrenke, A. Axmann, K. Eisele, W. Haydl, and J. Schneider, *Appl. Phys. Lett.* **46**, 381 (1985).
- ¹⁰A. Taguchi, K. Takahei, M. Matsuoka, and S. Tohno, *J. Appl. Phys.* **84**, 4471 (1998).
- ¹¹G. Franzo, F. Priolo, S. Coffa, A. Polman, and A. Carnera, *Appl. Phys. Lett.* **64**, 2235 (1994).
- ¹²B. Zheng, J. Michel, F. Y. G. Ren, L. C. Kimerling, D. C. Jacobson, and J. M. Poate, *Appl. Phys. Lett.* **64**, 2842 (1994).
- ¹³C.-X. Du, W.-X. Ni, K. B. Joelsson, and G. V. Hansson, *Appl. Phys. Lett.* **71**, 1023 (1997).
- ¹⁴N. A. Sobolev, A. M. Emel'yanov, and K. F. Shtel'makh, *Appl. Phys. Lett.* **71**, 1930 (1997).
- ¹⁵M. Markmann, E. Neufeld, A. Sticht, K. Brunner, and G. Abstreiter, *Appl. Phys. Lett.* **78**, 210 (2001).
- ¹⁶M. E. Castagna, S. Coffa, M. Monaco, A. Muscara, L. Caristia, S. Lorenti, and A. Messina, *Mater. Sci. Eng., B* **105**, 83 (2003).
- ¹⁷A. Karim, W.-X. Ni, A. Elfving, P. O. Å. Persson, and G. V. Hansson, *Mater. Res. Soc. Symp. Proc.* **866**, V4.2.1/FF4.2.1 (2005).
- ¹⁸G. V. Hansson, W.-X. Ni, C.-X. Du, A. Elfving, and F. Duteil, *Appl. Phys. Lett.* **78**, 2104 (2001).
- ¹⁹A. M. Emel'yanov, N. A. Sobolev, and A. N. Yakimenko, *Appl. Phys. Lett.* **72**, 1223 (1998).
- ²⁰M. S. Bresler, O. B. Gusev, O. E. Pak, and I. N. Yassievich, *Appl. Phys. Lett.* **75**, 2617 (1999).
- ²¹V. B. Shmagin, A. V. Lyutov, D. Yu. Reizov, K. E. Kudryavtsev, M. V. Stepikhova, and Z. F. Krasilnik, *Mater. Sci. Eng., B* **146**, 256 (2008).
- ²²C.-X. Du, W.-X. Ni, K. B. Joelsson, F. Duteil, and G. V. Hansson, *J. Lumin.* **80**, 329 (1998).
- ²³A. Karim, G. V. Hansson, and M. K. Linnarsson, *J. Phys.: Conf. Ser.* **100**, 042010 (2008).
- ²⁴J. F. M. Dignonnet, *Rare-Earth-Doped Fiber Laser and Amplifiers* (Dekker, New York, 2001).